SCIENTIFIC REPORTS

OPEN

New experimental evidence to support roaming in the reaction Cl + isobutene (i-C$_4$H$_8$)

Li-Wei Chen[1], Ching-Ming Hung[1], Hiroyuki Matsui[1] & Yuan-Pern Lee[1,2]

The reaction Cl + isobutene (i-C$_4$H$_8$) was reported by Suits *et al.* to proceed via, in addition to abstraction, an addition-elimination path following a roaming excursion of Cl; a near-zero translational energy release and an isotropic angular distribution observed at a small collision energy characterized this mechanism. We employed a new experimental method to further characterize this roaming mechanism through observation of the internal distribution of HCl (v, J) and their temporal behavior upon irradiation of a mixture of Cl$_2$C$_2$O$_2$ and i-C$_4$H$_8$ in He or Ar buffer gas. With 1–3 Torr buffer gas added to approach the condition of small collision energy, the intensities of emission of HCl (v = 1, 2) and the HCl production rates increased significantly; Ar shows a more significant effect than He because Ar quenches Cl more efficiently to reduce the collisional energy and facilitate the roaming path. According to kinetic modeling, the rate of addition-elimination (roaming) increased from $k_E \approx 2 \times 10^5 \, s^{-1}$ when little buffer gas was present to $\sim 1.9 \times 10^6 \, s^{-1}$ when 2–3 Torr of Ar was added, and the branching ratio for formation of [HCl (v = 2)]/[HCl (v = 1)] increased from 0.02 ± 0.01 for abstraction to 0.06 ± 0.01 for roaming.

The reactions of atomic chlorine (Cl) with alkenes (C$_n$H$_{2n}$) play important roles in the chemistry of the troposphere[1–5]. These reactions are also of fundamental importance in understanding the reaction kinetics or dynamics that involve a competition between various paths and a site selectivity. The two most significant channels of the primary Cl + C$_n$H$_{2n}$ reactions are the addition of a Cl atom to the C=C double bond to form a thermally stabilized adduct, chloroalkyl radical (•C$_n$H$_{2n}$Cl), and the metathesis reaction to form HCl and an alkyl radical (•C$_n$H$_{2n-1}$); the metathesis includes a direct abstraction of a H atom of the alkene by the Cl atom and an elimination of HCl from the energetic adduct •C$_n$H$_{2n}$Cl[6]. It is generally accepted that the abstraction dominates at low pressure, whereas the addition-stabilization mechanism becomes more important at high pressure[6–8].

Employing crossed molecular beams to investigate the dynamics of the reaction Cl + i-C$_4$H$_8$, Suits and coworkers detected C$_4$H$_7$ with a slice ion-imaging method[9,10]. These authors found that the addition-elimination path occurs from an abstraction-like Cl-H-C geometry rather than a conventional three-center or four-center transition state, and this geometry is attained through roaming excursions of the Cl atom from the initially formed adduct. The experimental observations to support this roaming mechanism are limited: a release of translational energy with a maximal distribution near zero energy and a fully isotropic angular distribution of C$_4$H$_7$ product were observed when a small collisional energy was employed.

Preston *et al.* employed velocity-map imaging to measure the quantum states and velocity of HCl produced from reactions Cl + propene, i-C$_4$H$_8$, and dimethylbutene; signals from both direct abstraction and addition-elimination were observed[11]. These authors simulated trajectories that indicated the importance of a large-amplitude excursion of the Cl atom far from equilibrium geometry within the chloroalkyl complex, which ultimately led to formation of HCl + allyl fragmentation[12], but a clear distinction in the internal energy distribution of HCl produced via abstraction from that via addition-elimination of Cl + i-C$_4$H$_8$ was unavailable.

Roaming dynamics that involve reactions of a radical (or an atom) with a radical, resulting typically from photofragmentation of a suitable precursor, are now widely recognized as an important path in unimolecular decompositions[13–17], but their roles in radical (or an atom) - molecule reactions remain less certain. Molecular dynamics simulations of the unimolecular dissociation of energetic C$_2$H$_4$OH radicals reveal a minor roaming channel of OH + C$_2$H$_4$ that leads to formation of H$_2$O and C$_2$H$_3$[18]. Roaming was observed in photolysis of NO$_3$

[1]Department of Applied Chemistry and Institute of Molecular Science, National Chiao Tung University, 1001 Ta-Hsueh Rd., Hsinchu 30010, Taiwan. [2]Institute of Atomic and Molecular Sciences, Academia Sinica, Taipei 10617, Taiwan. Correspondence and requests for materials should be addressed to Y.-P.L. (email: yplee@mail.nctu.edu.tw)

Set	Conditions[a]		Experiment		Kinetic fit of HCl ($v=1$) and HCl ($v=2$)				
	$P_{i\text{-}C_4H_8}$/Torr	P_M/Torr	y^b	$\frac{[HCl(v=2)]}{[HCl(v=1)]}$	$k_E/10^5\,s^{-1}$	$k_{rev}/10^5\,s^{-1}$	$k_q/10^5\,s^{-1}$	ϕ_2/ϕ_1 (abs.)	$\varepsilon_2/\varepsilon_1$ (elim.)
A	0.213	0.010 (Ar)	0.06	0.015 ± 0.004	0.5	19.8	0.6	0.00 (0.02)^c	0.23
	0.482	0.010 (Ar)	0.20	0.024 ± 0.004	2.4	43.5	1.0	0.05 (0.03)	0.00
	0.687	0.011 (Ar)	0.17	0.023 ± 0.005	2.1	63.4	1.5	0.01 (0.03)	0.20
	0.914	0.011 (Ar)	0.16	0.026 ± 0.007	1.5	85.6	2.1	0.05 (0.04)	0.00
B	0.224	0.940 (He)	0.57	0.035 ± 0.002	9.0	11.4	1.0	0.04 (0.02)	0.04
	0.225	1.910 (He)	0.47	0.034 ± 0.002	8.8	10.9	1.1	0.00 (0.02)	0.06
	0.226	2.990 (He)	0.37	0.031 ± 0.002	7.8	10.9	1.2	0.00 (0.01)	0.06
C	0.224	0.940 (Ar)	0.75	0.035 ± 0.002	10.9	9.5	1.2	0.00 (0.00)	0.05
	0.225	1.910 (Ar)	0.72	0.038 ± 0.001	19.6	0.0	2.1	0.00 (0.00)	0.05
	0.226	2.990 (Ar)	1.00	0.045 ± 0.001	18.7	0.0	3.1	0.01 (0.05)	0.07

Table 1. Experimental conditions, relative intensities y of HCl, observed ratios of [HCl($v=2$)]/ [HCl($v=1$)], fitted rate coefficients of elimination k_E and their associated k_{rev}, rate coefficient of quenching k_q, branching ratios for formation of HCl ($v=2$) over HCl ($v=1$) ϕ_2/ϕ_1 (from abstraction) and $\varepsilon_2/\varepsilon_1$ (from elimination) in three sets of experiments. ^{a}Partial pressure of $Cl_2C_2O_2$ is 10–11 mTorr. ^{b}Intensity of HCl relative to that from the experiment with $P_{Ar} = 2.99$ Torr. ^{c}Fitted results with $\varepsilon_2/\varepsilon_1$ fixed at 0.05 are listed in parentheses.

via both ground- and excited-state surfaces to form NO + O_2 and supported by theoretical calculations[19–22]. Both these reactions are initiated from photodissociation of free radicals; reported roaming reaction initiated from reactions of radical (atom) and molecule is rare.

In the roaming mechanism of Cl + i-C_4H_8, because the reaction to form HCl + C_4H_7 has a small exothermicity (~68 kJ mol^{-1}) and because the addition-elimination path occurs at the abstraction-like near-linear Cl−H−C geometry, to distinguish the internal distributions of HCl produced via abstraction from that via the addition-roaming-elimination path is difficult. In this work we demonstrate a new experimental method to characterize the roaming path in the atom-molecule reaction Cl + i-C_4H_8 → HCl + C_4H_7 by using a step-scan Fourier-transform infrared (FTIR) spectrometer to obtain time-resolved IR emission spectra of HCl[23–25].

Results and Discussion
Emission spectra of HCl. According to the results of Joalland *et al.*[9,10], roaming of Cl + i-C_4H_8 was most prominent at a small collisional energy (~17 kJ mol^{-1}). Because the Cl atoms produced upon photolysis still have significant kinetic energy, collisional quenching to a nearly thermal distribution of kinetic energy is expected to enhance the roaming path. We hence compared the effect of adding He or Ar up to a total pressure of 3 Torr to quench the kinetic energy of Cl atoms after photolysis.

Similar experiments with the same amount of $Cl_2C_2O_2$ (10–11 mTorr) and laser fluence were performed for three sets of data; the conditions are listed in Table 1. Set A was for investigation of the dependence on the concentration of i-C_4H_8 with little buffer gas, set B was for investigation of the effect of adding He as a quencher, and set C was for investigation of the effect of adding Ar as a quencher. The absorption cross section of $Cl_2C_2O_2$ at 248 nm is ~3.1×10^{-19} cm^2 molecule^{-1}[26]. Typically, ~13% of $Cl_2C_2O_2$ was photodissociated with a fluence of 343 mJ cm^{-2}.

Emission spectra of HCl at resolution 0.7 cm^{-1} recorded 0–5 μs after photolysis of $Cl_2C_2O_2$ (~11 mTorr), i-C_4H_8 (~220 mTorr), and Ar (0.010 and 2.99 Torr) are presented in Fig. 1(a,b), respectively; lines of H^{35}Cl and H^{37}Cl are well resolved. The vibration-rotational assignments of each line based on spectral parameters reported by Arunan *et al.*[27] and Coxon and Roychowdhury[28] are shown as sticks for transitions of $v'=1$, $J'\leq13$ and $v'=2$, $J'\leq10$. At ~3.2 Torr, formation of the HCl ($v=2$) was enhanced slightly, as shown in Fig. 1(b). For comparison, Preston *et al.* observed $v'=1$, $J'\leq7$ and $v'=2$, $J'=1$ in their jet experiments using velocity-map ion imaging[11]. The energetics, discussed in Supplementary Sec. A, indicate that the available energy for formation of HCl + C_4H_7 is ~81 kJ mol^{-1} (6770 cm^{-1}) when Cl atoms are thermalized by collisions with Ar or He; this energy is close to the energy of HCl ($v=2$, $J=10$) at 6743 cm^{-1}.

Rotational temperature. The rotational distributions of HCl are Boltzmann, as shown in Supplementary Fig. S1 for spectra recorded 0–1 μs after photolysis. Derivation of nascent rotational temperature is discussed in Supplementary Sec. B. Nascent rotational temperatures and average rotational energies observed in three sets of experiments are listed in Supplementary Table S1. In all cases, the rotational temperatures are similar (deviations within 15%) and decrease slightly from ~370 K to ~340 K as the pressure increases to ~3.2 Torr; detailed data are in Supplementary Table S1. The average rotational energy is hence ~3 kJ mol^{-1}, independent of pressure. The small rotational energy indicates that, if roaming occurs more significantly at greater pressure, the HCl product generated from this path has rotational excitation similar to that from abstraction. This condition is consistent with a prediction that the roaming (addition-elimination) path occurs from the abstraction-like near-linear Cl-H-C geometry[9].

Vibrational excitation and relative intensity of HCl. Because only HCl ($v=1$) and HCl ($v=2$) were observed, to determine accurately the vibrational temperature and energy is difficult. We list $P_{v=2}/P_{v=1}$ and the relative intensity y of HCl ($v=1$ and 2) in various experiments in Table 1; the relative intensity was
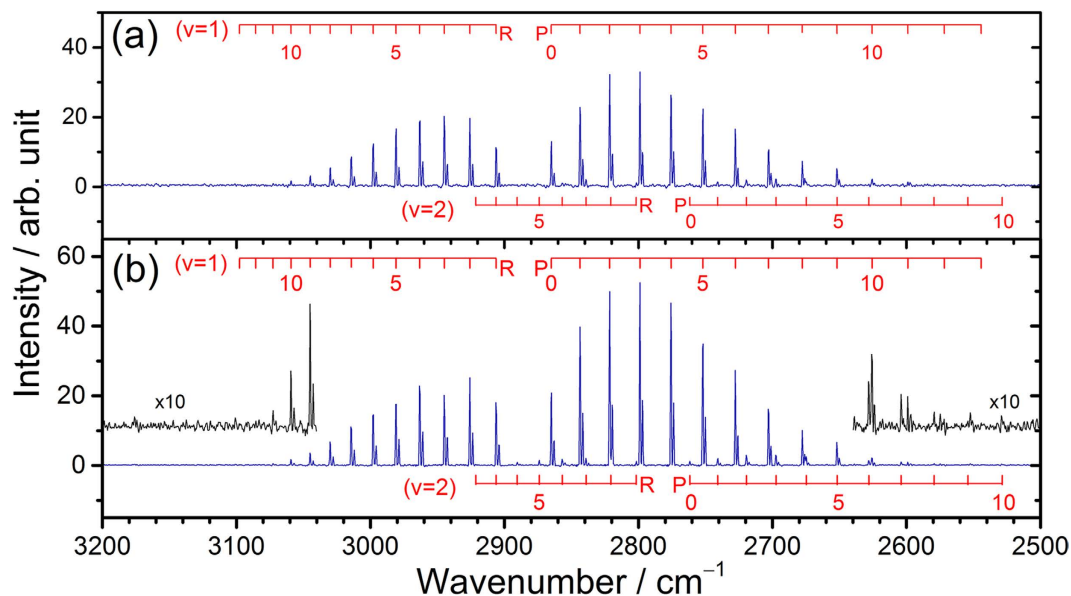
Figure 1. Emission spectra of HCl in spectral region 2500–3200 cm^{-1} recorded 0–5 μs after photolysis at 248 nm. (**a**) A flowing mixture of $Cl_2C_2O_2$ (10 mTorr), i-C_4H_8 (213 mTorr) and Ar (10 mTorr). (**b**) A flowing mixture of $Cl_2C_2O_2$ (11 mTorr), i-C_4H_8 (226 mTorr) and Ar (2.99 Torr). Spectral resolution is 0.7 cm^{-1}. The assignments are shown as sticks; numbers indicate rotational quantum number J'.

compared to the results of $P_T = 3.23$ Torr (Ar) in set C. When little buffer gas was present, [HCl ($v=2$)]/[HCl ($v=1$)] $= 0.015 \pm 0.004$, whereas when ~3 Torr of Ar was added, [HCl ($v=2$)]/[HCl ($v=1$)] $= 0.045 \pm 0.001$. Because of the excellent ratio of signal to noise in the spectra, the error in the determination of relative population was estimated to be less than 25% of the value when the signal is small; the difference in these ratios is hence significant, as can also be seen from the consistency in ratios determined in various experiments (Table 1). The small difference is partly because the abstraction path still contributes when the buffer gas was added and partly because the difference in [HCl ($v=2$)]/[HCl ($v=1$)] between abstraction and addition-elimination is not so large. Nevertheless, the vibrational excitation of HCl was clearly enhanced when the buffer gas was added.

Because we could not measure the population of HCl ($v=0$), these relative intensities consequently provide only a rough estimate of the extent of HCl produced. Nevertheless, it is clear from Table 1 that the intensity of (vibrationally excited) HCl was enhanced by as much as 16 times when a buffer gas was added, and adding Ar showed a greater enhancement than adding He.

Rate coefficient derived from kinetic fitting of vibrational temporal profiles.

Because the rotational temperature of HCl is near 360 K and independent of pressure, the rotational temporal profile provides little information about the kinetics of the reaction. We thus analyzed only the vibrational temporal profiles; some representative plots in experimental set A for $P_T = 0.23$ Torr, set B for $P_T = 3.23$ Torr (He), and set C for $P_T = 3.23$ Torr (Ar) are shown in Fig. 2. Temporal profiles for other experiments in sets A–C are presented in Supplementary Figs S2–S4, respectively.

We consider the reaction mechanism depicted in Fig. 3. The reaction of Cl + i-C_4H_8 forms energetic adduct $ClC_4H_8^*$ with a rate coefficient k_{for}; $ClC_4H_8^*$ might be stabilized by collision with the third-body M (rate coefficient k_M [M]), dissociate back to the reactants (rate coefficient k_{rev}), or eliminate HCl via roaming-elimination (rate coefficient k_E). The abstraction and elimination channels might produce HCl with distinct vibrational distributions. The abstraction reaction (rate coefficient k_{abs}) has three channels to produce HCl ($v=0$), HCl ($v=1$), and HCl ($v=2$) with branching ratios ϕ_0, ϕ_1, and ϕ_2, respectively. The elimination reaction has, similarly, three channels with branching ratios ε_0, ε_1, ε_2 for production of HCl ($v=0$–2), respectively. The decay rate coefficients $k_{q(v)}$ are also separated for each vibrational level of HCl and include both quenching and loss. The solution of [HCl(t)] contains three exponential terms, but they are complex functions of rate coefficients, as discussed in Supplementary Sec. C. Hence, instead of fitting the temporal profiles to three exponential terms, we simulated the temporal profile with given rate coefficients and compare with experimental results. We systematically varied the rate coefficients using mathematical tools to derive the best fit between the experimental data and the simulated temporal profiles with the least deviations.

Because eight rate coefficients are involved in this mechanism, it is unlikely to derive a unique fit of these parameters from the temporal profiles. We thus fixed some well-known rate coefficients and varied only k_E and k_{rev}, and the vibrational branching ratios of abstraction (ϕ_2/ϕ_1) and elimination ($\varepsilon_2/\varepsilon_1$) reactions. The total rate coefficient k_T for reaction Cl + i-C_4H_8 at 1 bar (air) was determined to be $k_T = (3.40 \pm 0.28) \times 10^{-10}$ cm^3 molecule^{-1} s^{-1} by Ezell *et al.*[29]. Following the empirical additivity rules based on data of reactions of Cl with alkanes and alkenes, these authors proposed that $k_{abs} = 6.8 \times 10^{-11}$ cm^3 molecule^{-1} s^{-1} for the formation of HCl and $k_{add} = 2.7 \times 10^{-10}$ cm^3 molecule^{-1} s^{-1} for the formation of stabilized ClC_4H_8; the value of k_{abs} should be k_{meta}, rate coefficient
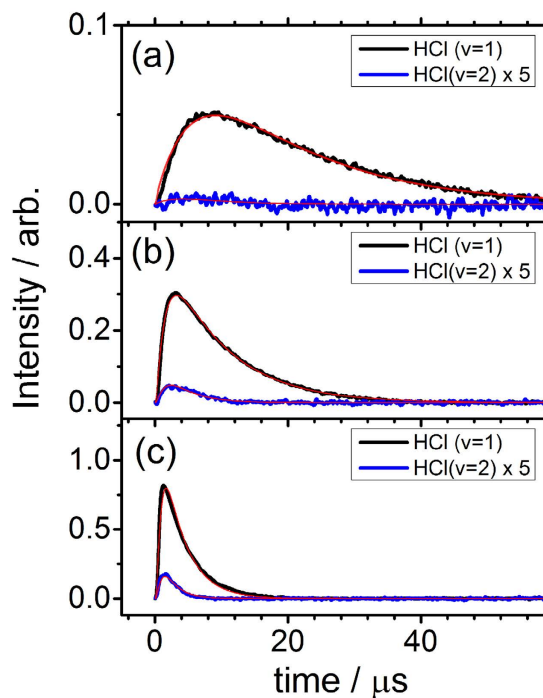
Figure 2. Comparison of observed temporal profiles of HCl (v) with simulations. (a) A flowing mixture of $Cl_2C_2O_2$ (10 mTorr), i-C_4H_8 (213 mTorr) and Ar (10 mTorr). **(b)** A flowing mixture of $Cl_2C_2O_2$ (10 mTorr), i-C_4H_8 (226 mTorr) and He (2.99 Torr). **(c)** A flowing mixture of $Cl_2C_2O_2$ (10 mTorr), i-C_4H_8 (226 mTorr) and Ar (2.99 Torr). HCl ($v=1$) is in black and HCl ($v=2$), multiplied by a factor of 5, is in blue. The kinetic simulations are in red.
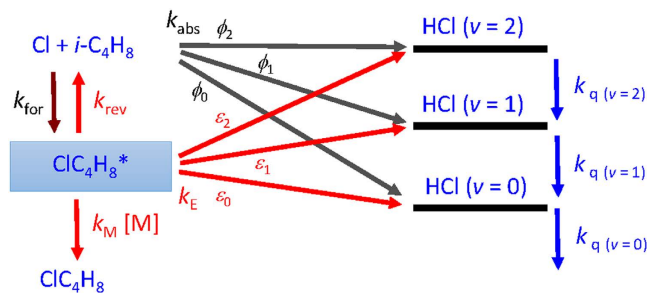
Figure 3. Reaction mechanism of Cl + i-C_4H_8.

of metathesis, that includes abstraction and addition-elimination. Considering that abstraction reactions occur only on the methyl groups of propene and isobutene, one estimates $k_{abs} = 4.6 \times 10^{-11}$ cm³ molecule⁻¹ s⁻¹ because i-C_4H_8 has two methyl moieties and k_{abs} was determined to be 2.3×10^{-11} cm³ molecule⁻¹ s⁻¹ for Cl + propene[7]. The value of k_{for} for the reaction Cl + i-C_4H_8 can be taken as the difference between total rate coefficient k_T and k_{abs}, that is, $k_{for} = 2.94 \times 10^{-10}$ cm³ molecule⁻¹ s⁻¹, which corresponds satisfactorily with the value for Cl + propene, $k_\infty = (2.7 \pm 0.4) \times 10^{-10}$ cm³ molecule⁻¹ s⁻¹. The rate coefficient at the low-pressure limit for Cl + i-C_4H_8 is unreported, but the corresponding value for Cl + propene is $k_0 = (4.0 \pm 0.4) \times 10^{-28}$ cm⁶ molecule⁻² s⁻¹[7]. If we assume that the termolecular reaction Cl + i-C_4H_8 + M to form ClC$_4$H$_8$ is still in the linear regime for $P_T \leq 3$ Torr, and use k_0 of the reaction of Cl + propene for Cl + i-C_4H_8, $k_M = (4.0 \pm 0.4) \times 10^{-28}$ [i-C_4H_8] [M] cm⁶ moleule⁻² s⁻¹.

Because HCl ($v=0$) is unobserved in emission, we fit only the temporal profiles of HCl ($v=1$) and HCl ($v=2$) simultaneously on varying k_q, ϕ_2/ϕ_1, k_E, and $\varepsilon_2/\varepsilon_1$ to derive the best fit between the experimental data and the simulated temporal profiles. In these fits, $k_{abs} = 4.6 \times 10^{-11}$ cm³ molecule⁻¹ s⁻¹, $k_{for} = 2.9 \times 10^{-10}$ cm³ molecule⁻¹ s⁻¹, $k_M = 4.0 \times 10^{-28}$ [i-C_4H_8] [M] cm⁶ molecule⁻² s⁻¹ were fixed, and $k_{rev} + k_M + k_E = k_{for}$ [i-C_4H_8]. The representative fitted temporal profiles of HCl (v) for experiments in set A (0.22 Torr), set B (3.23 Torr), and set C (3.23 Torr, Ar) are shown in Fig. 2; additional profiles are shown in Supplementary Figs S2–S4. We plot k_E as a function of density [M] of i-C_4H_8 or He or Ar in Fig. 4 for experimental sets A–C. Fitted results of k_E, k_q, ϕ_2/ϕ_1, and $\varepsilon_2/\varepsilon_1$ are listed in Table 1.
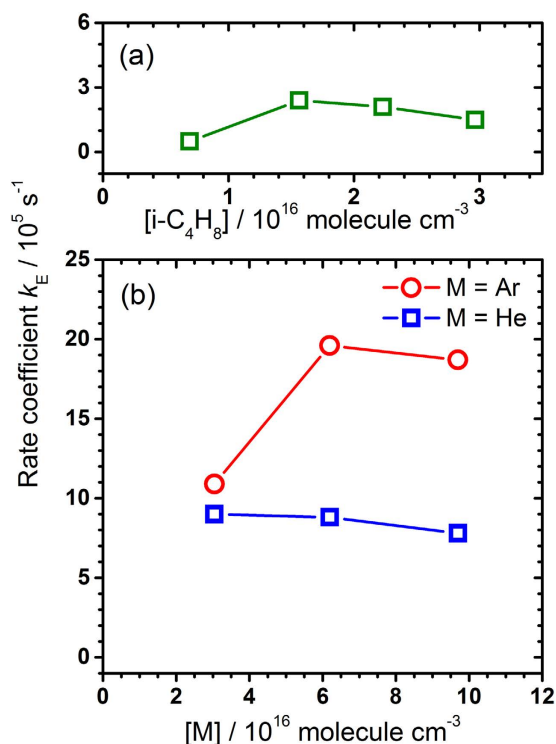
Figure 4. Fitted k_E in three sets of experiments. (a) A flowing mixture of $Cl_2C_2O_2$ (10 mTorr), Ar (10 mTorr), and i-C_4H_8 (213–914 mTorr). **(b)** A flowing mixture of $Cl_2C_2O_2$ (10 mTorr), i-C_4H_8 (226 mTorr) and buffer gas He (0.94–2.99 Torr, symbol □) or Ar (0.94–2.99 Torr, symbol ○).

For experiments in set A with varying i-C_4H_8 and little buffer gas, k_E remains small and is nearly constant with $k_E = (1.6 \pm 0.8) \times 10^5\,s^{-1}$ (Fig. 4(a)). For He as a buffer gas, k_E is much greater than those without buffer gas and remains nearly constant with $k_E = (8.5 \pm 0.7) \times 10^5\,s^{-1}$ for [He] $= (3.0–9.7) \times 10^{16}$ molecule cm^{-3}, whereas k_E increases from $1.1 \times 10^5\,s^{-1}$ at [Ar] $= 3.0 \times 10^{16}$ molecule cm^{-3} to $(1.9 \pm 0.1) \times 10^6\,s^{-1}$ at [Ar] $= (6.2–9.7) \times 10^{16}$ molecule cm^{-3} (Fig. 4(b)). Such a significant increase in k_E for experiments with an added quencher, especially Ar, can be explained only with an enhanced addition-elimination channel induced by the collisional quenching of the kinetic energy of Cl; because the mass of Ar is similar to that of Cl, Ar is a much more efficient quencher than He for kinetic energy of Cl.

Detailed sensitivity and error analysis are available in Supplementary Sec. D. The deviations derived in these analysis are much smaller than the enhancement of k_E observed in experimental sets B and C as compared to those in experiments with little buffer gas.

For experimental sets B and C (in which roaming is more important), $\varepsilon_2/\varepsilon_1$ are consistent with average (5.5 ± 0.9) %. We thus fixed $\varepsilon_2/\varepsilon_1 = 0.06$ to fit the data once more; a much more consistent value of ϕ_2/ϕ_1 with average (3.0 ± 0.7) % for set A (in which abstraction is more important) was derived, as shown in parentheses in Table 1 (other fitted parameters are listed in Supplementary Table S2). The ϕ_2/ϕ_1 value of 0.02 when little buffer gas was added is the smallest and is taken as the ϕ_2/ϕ_1 value for abstraction. This value is consistent with the average ratio of $[HCl(v=2)]/[HCl(v=1)] = 0.022$ in experimental set A derived from integrated intensities. The ratio of $\varepsilon_2/\varepsilon_1 = 0.06 \pm 0.01$ for roaming, derived from kinetic fitting, is greater than values $[HCl(v=2)]/[HCl(v=1)] = 0.035–0.045$ in experimental set C because the latter values include contributions from both abstraction and roaming.

These results indicate that the roaming path generates more vibrationally excited HCl than the abstraction path, consistent with the expectation according to consideration of the structures of the transition states, because the roaming transition state has an H−Cl distance of 2.37 Å[9], much greater than the H−Cl distance of 1.59 Å for the transition state of H-abstraction[30] and the equilibrium distance 1.275 Å of HCl. In the case of photolysis of acetaldehyde, the roaming transition state has a C−H distance of 1.722 Å, much greater than the equilibrium C−H distance of 1.093 Å of CH_4[31]. The CH_4 product after roaming of CH_3 around HCO was found to have extreme significant vibrational excitation, with the vibrational distribution peaked at ~95% of the total available energy[32]. For the reaction of Cl + i-C_4H_8, the average available energy for formation of HCl + C_4H_7 is ~81 kJ mol^{-1} (6770 cm^{-1}) when Cl atoms are thermalized by collisions with Ar or He. This energy can populate HCl only up to $v=2$, $J=10$, so the extent of vibrational excitation is not as great as that of the roaming of CH_3 + HCO.

This competition between abstraction and addition-elimination via a long-lived complex is similar to the early work on H + ICl by Polanyi et al.[33]. In their 3D trajectory studies, they reported that the HCl formed with a small internal energy resulted from reaction of H directly at the Cl-end of ICl, whereas the HCl formed with high internal energy was produced by migration of H from the I-site to the Cl-site, following a lingering interaction of H with I.

Conclusion

In summary, experimental evidence of three types supports the involvement of the roaming mechanism that is expected to be enhanced at small collisional energy as more buffer gas is added to thermalize the kinetic energy of Cl after photolysis; Ar is expected to be more effective than He in quenching the kinetic energy of Cl. The evidence follows. (1) The intensity of HCl ($v = 1$ and 2) was enhanced by as much as sixteen times when buffer gas at 1–3 Torr was added, more so when the same amount of Ar than when He was added. (2) The observed temporal profiles indicate a significantly increased rate for the formation of HCl when the buffer gas was added; Ar was more effective than He. According to the kinetic modeling, the rate of addition-elimination (roaming) increased from $k_E \approx 2 \times 10^5 \, \text{s}^{-1}$ when little buffer gas was present to $\sim 8.5 \times 10^5 \, \text{s}^{-1}$ when 1–3 Torr of He was added, and $\sim 1.9 \times 10^6 \, \text{s}^{-1}$ when 2–3 Torr of Ar was added. (3) Ratio [HCl ($v = 2$)]/[HCl ($v = 1$)] increased when Ar (1–3 Torr) was added relative to when little buffer gas was present. According to the kinetic modeling, we derived a branching ratio $\varepsilon_2/\varepsilon_1 = 0.06 \pm 0.01$ from roaming and $\phi_2/\phi_1 = 0.02 \pm 0.01$ from abstraction. This result is consistent with an expectation that HCl produced from the roaming mechanism to have greater vibrational excitation, even though the excitation is limited by the small exothermicity.

The rotational temperature of HCl near 360 K shows no significant variation under varied pressure, indicating that the rotational excitation of HCl from abstraction and roaming is similarly small, consistent with the proposal that roaming (addition-elimination) occurs from the abstraction-like linear Cl-H-C geometry.

Methods

The step-scan Fourier-transform infrared (FTIR) spectrometer coupled with a set of Welsh mirrors to obtain time-resolved IR emission spectra has been described[23–25]. A gaseous flowing mixture of isobutene and oxalyl chloride ($Cl_2C_2O_2$) was irradiated with an excimer laser at 248 nm for production of Cl to initiate the reaction of $Cl + i\text{-}C_4H_8$. We used $Cl_2C_2O_2$ instead of Cl_2 as a source of Cl atoms because the secondary reactions of C_4H_7 with Cl_2 might interfere.

The sizes of the photolysis beams at the detection center were $\sim 11.0 \times 5.7 \, \text{mm}^2$ with a fluence $345-380 \, \text{mJ cm}^{-2}$ from a KrF laser (Coherent, COMPexPro-50) at 248 nm. The transient signal detected with an InSb detector (rise time 0.22 μs) was further amplified 20–160 times (bandwidth 1 MHz) before being digitized and recorded with an external data-acquisition board (12-bit) at resolution 25 ns. For survey spectra, data were typically averaged over 60 laser pulses at each scan step; 1332 scan steps were performed to yield an interferogram resulting in a spectrum in a region 1800–7800 cm^{-1} at resolution 12 cm^{-1}. To detect emission of HCl, we used undersampling with two IR filters (Spectrogon SP-4300 and OCLI W03999-4) to allow passage of light in the region $2350-3250 \, \text{cm}^{-1}$. Data were typically averaged over 30 laser pulses at each scan step; 3578 scan steps were performed to yield an interferogram resulting in a spectrum of resolution 0.7 cm^{-1}. To improve the ratio of signal to noise (S/N) of the spectra of HCl, four spectra recorded under nearly the same experimental conditions were averaged. To improve further the S/N ratio, n consecutive time-resolved spectra were summed to yield spectra representing emission at intervals of $n \times 25$ ns; typically $n = 40$ and spectra at 1-μs intervals were used.

Samples of $Cl_2C_2O_2$ and Ar (or He) were injected into the vacuum chamber as a diffusive beam through a slit-shaped inlet. The $i\text{-}C_4H_8$ sample has vapor pressure ~ 340 Torr at 298 K. Additional He or Ar in a minimal pressure (~ 10 mTorr) was added near the entrance of the photolysis port to suppress the formation of a solid deposit on the quartz window. The partial pressures of each species were calculated by the flow rates of each species, the total flow rate, and the total pressure.

$Cl_2C_2O_2$ (>98%, Lancaster) and $i\text{-}C_4H_8$ (99%, Sigma-Aldrich) were purified using the freeze-pump-thaw method. Ar (Specialty Gases of America, 99.9995%) and He (Specialty Gases of America, 99.9995%) were used as received.

References

1. Finlayson-Pitts, B. J. & Pitts, J. N. *Chemistry of the Upper and Lower Atmosphere—Theory, Experiments, and Applications* (Academic Press, San Diego, CA, *USA*, 2000).
2. Singh, H. B. & Kasting, J. F. Chlorine-hydrocarbon photochemistry in the marine troposphere and lower stratosphere. *J. Atmos. Chem.* **7,** 261–285 (1988).
3. Walavalkar, M. *et al.* Cl atom initiated oxidation of 1-alkenes under atmospheric conditions. *Atoms. Environ.* **67,** 93–100 (2013).
4. Timerghazin, Q. K. & Ariya, P. A. Kinetics of the gas phase reactions of atomic chlorine with selected monoterpenes. *Phys. Chem. Chem. Phys.* **3,** 3981–3986 (2001).
5. Atkinson, R. & Arey, J. Gas-phase tropospheric chemistry of biogenic volatile organic compounds: a review. *Atmos. Environ.* **37,** 197–219 (2003).
6. Taatjes, C. A. Time-resolved infrared absorption measurements of product formation in Cl atom reactions with alkenes and alkynes. *Int. Rev. Phys. Chem.* **18,** 419–458 (1999).
7. Kaiser, E. W. & Wallington, T. J. Pressure dependence of the reaction $Cl + C_3H_6$. *J. Phys. Chem.* **100,** 9788–9793 (1996).
8. Pilgrim, J. S. & Taatjes, C. A. Infrared absorption probing of the $Cl + C_3H_6$ reaction: rate coefficients for HCl production between 290 and 800 K. *J. Phys. Chem. A* **101,** 5776–5782 (1997).
9. Joalland, B., Shi, Y., Kamasah, A., Suits, A. G. & Mebel, A. M. Roaming dynamics in radical addition–elimination reactions. *Nat. Commun.* **5,** 4064 (2014).
10. Joalland, B., Camp, R. V., Shi, Y., Patel, N. & Suits, A. G. Crossed-beam slice imaging of Cl reaction dynamics with butene isomers. *J. Phys. Chem. A* **117,** 7589–7594 (2013).
11. Preston, T. J., Dunning, G. T., Orr-Ewing, A. J. & Vázquez, S. A. Direct and indirect hydrogen abstraction in Cl + alkene reactions. *J. Phys. Chem. A* **118,** 5595–5607 (2014).
12. Hornung, B., Preston, T. J., Pandit, S., Harvey, J. N. & Orr-Ewing, A. J. Computational study of competition between direct abstraction and addition-elimination in the reaction of Cl atoms with propene. *J. Phys. Chem. A* **119,** 9452–9464 (2015).
13. Goncharov, V., Herath, N. & Suits, A. G. Roaming dynamics in acetone dissociation. *J. Phys. Chem. A* **112,** 9423–9428 (2008).
14. Suits, A. G. Roaming atoms and radicals: a new mechanism in molecular dissociation. *Acc. Chem. Res.* **41,** 873–881 (2008).
15. Hause, M. L., Herath, N., Zhu, R., Lin, M. & Suits, A. G. Roaming-mediated isomerization in the photodissociation of nitrobenzene. *Nat. Chem.* **3,** 932–937 (2011).
16. Bowman, J. M. & Shepler, B. C. Roaming radicals. *Annu. Rev. Phys. Chem.* **62,** 531–553 (2011).

17. Bowman, J. M. Roaming. *Mol. Phys.* **112,** 2516–2528 (2014).
18. Kamarchik, E., Koziol, L., Reisler, H., Bowman, J. M. & Krylov A. I. Roaming pathway leading to unexpected water + vinyl products in C$_2$H$_4$OH dissociation. *J. Phys. Chem. Lett.* **1,** 3058–3065 (2010).
19. Grubb, M. P., Warter, M. L., Suits, A. G. & North, S. W. Evidence of roaming dynamics and multiple channels for molecular elimination in NO$_3$ photolysis. *J. Phys. Chem. Lett.* **1,** 2455–2458 (2010).
20. Grubb, M. P. *et al.* No straight path: roaming in both ground- and excited-state photolytic channels of NO$_3$ → NO + O$_2$. *Science* **335,** 1075–1078 (2012).
21. Grubb, M. P., Warter, M. L., Johnson, K. M. & North, S. W. Ion imaging study of NO$_3$ radical photodissociation dynamics: characterization of multiple reaction pathways. *J. Phys. Chem. A* **115,** 3218–3226 (2011).
22. Fernando, R. *et al.* Visible/Infrared dissociation of NO$_3$: roaming in the dark or roaming on the ground. *J. Phys. Chem. A* **119,** 7163–7168 (2015).
23. Lin, S.-R. & Lee, Y.-P. Photodissociation of 1,1-Difluoroethene(CH$_2$CF$_2$) at 193 nm monitored with step-scan time-resolved Fourier-transform infrared emission spectroscopy. *J. Chem. Phys.* **111,** 9233–9241 (1999).
24. Wu, C.-Y., Lee, Y.-P., Ogilvie, J. F. & Wang, N. S. Photolysis of oxalyl chloride (ClCO)$_2$ at 248 nm: emission of CO($v' \leq 3$, $J' \leq 51$) detected with time-resolved Fourier-transform spectroscopy. *J. Phys. Chem. A* **107,** 2389–2393 (2003).
25. Lee, P.-W., Scrape, P. G., Butler, L. J. & Lee, Y.-P. Two HCl-elimination channels and two CO-formation channels detected with time-resolved infrared emission upon photolysis of acryloyl chloride [CH$_2$CHC(O)Cl] at 193 nm. *J. Phys. Chem. A* **119,** 7293–7304 (2015).
26. Ghosh, B., Papanastasiou, D. K. & Burkholder, J. B. Oxalyl chloride, ClC(O)C(O)Cl: UV/VIS spectrum and Cl atom photolysis quantum yields at 193, 248, and 351 nm. *J. Chem. Phys.* **137,** 164315 (2012).
27. Arunan, E., Setser, D. W. & Ogilvie, J. F. Vibration-rotational Einstein coefficients for HF/DF and HCl/DCl. *J. Chem. Phys.* **97,** 1734–1741 (1992).
28. Coxon, J. A. & Roychowdhury, U. K. Rotational analysis of the B$^1\Sigma^+$ → X$^1\Sigma^+$ system of H^{35}Cl. *Can. J. Phys.* **63,** 1485–1497 (1985).
29. Ezell, M. J., Wang, W., Ezell, A. A., Soskin, G. & Finlayson-Pitts, B. J. Kinetics of reactions of chlorine atoms with a series of alkenes at 1 atm and 298 K: structure and reactivity. *Phys. Chem. Chem. Phys.* **4,** 5813–5820 (2002).
30. Chu, G. *et al.* Investigation on addition and abstraction channels in Cl reactions with 1-butene and isobutene. *Int. J. Mass Spectrom.* **375,** 1–8 (2015).
31. Houston, P. L. & Kable, S. H. Photodissociation of acetaldehyde as a second example of the roaming mechanism. *Proc. Nat. Acad. Sci.* **103,** 16079–16082 (2006).
32. Heazlewood, B. R. *et al.* Roaming is the dominant mechanism for molecular products in acetaldehyde photodissociation. *Proc. Nat. Acad. Sci.* **105,** 12719–12724 (2008).
33. Polanyi, J. C., Schreiber, J. L. & Skrlac, W. J. Distribution of reaction products (theory) Part 12.—microscopic branching in H + XY → HX + Y, HY + X (X, Y = halogens). *Faraday Discuss. Chem. Soc.* **67,** 66–89 (1979).

Acknowledgements

Author Contributions

L.-W.C. wrote the program and performed the kinetic analysis. C.-M.H. performed the experiments and analyzed the spectra. H.M. conceived and designed the kinetic analysis. Y.-P.L. conceived and designed the experiments and wrote the paper.

Additional Information

Supplementary information accompanies this paper at http://www.nature.com/srep

Competing financial interests: The authors declare no competing financial interests.

How to cite this article: Chen, L.-W. *et al.* New experimental evidence to support roaming in the reaction Cl + isobutene (*i*-C$_4$H$_8$). *Sci. Rep.* **7,** 40105; doi: 10.1038/srep40105 (2017).

Publisher's note: Springer Nature remains neutral with regard to jurisdictional claims in published maps and institutional affiliations.